A One-Year Cloud Climatology Derived from the Micro Pulse Lidar

G. G. Mace
Department of Meteorology, University of Utah
Salt Lake City, Utah

E. E. Clothiaux and T. P. Ackerman
Department of Meteorology, Pennsylvania State University
University Park, Pennsylvania

J. D. Spinhirne and V. S. Scott
NASA/Goddard Space Flight Center
Greenbelt, Maryland

Abstract

A cloud detection algorithm that attempts to identify all of the significant power returns from the vertical column above the micro pulse lidar at all times was applied to one year of micro pulse lidar data collected at the U.S. Department of Energy (DOE) Atmospheric Radiation Measurement (ARM) Southern Great Plains (SGP) central facility near Lamont, Oklahoma. The results of this analysis are presented, and the potential significance of such long-term lidar measurements is considered.

Introduction

Cloud climatologies derived from surface-based active remote sensor data can address some of the ambiguities present in more conventional cloud observational records. For example, accurate and comprehensive climatologies of cloud occurrence as a function of location, height, and time are difficult to compile from satellite measurements and surface observers due to uncertainties in the interpretation of the former and to subjective biases in the latter. The use of ground-based active remote sensing for construction of cloud climatologies is on the threshold of becoming a reality. In the past, cloud profiling radars (Kropfli et al. 1995; Clothiaux et al. 1995) and lidars (Reagan et al. 1989) that can probe the entire troposphere were expensive and required staff for maintenance and operation. Consequently, the datasets generated by these instruments have tended to be of short duration and targeted at specific research issues (Winker and Vaughn 1994; Uttal et al. 1995). The installation of the micro pulse lidar at the DOE ARM SGP central facility represents the first operational use of a tropospheric lidar system. As one example of the potential value of the resulting data, we analyzed a 12-month record of cloud base heights from a combined micro pulse lidar and Belfort laser ceilometer dataset. We compiled cloud base height frequency-of-occurrence histograms as a function of the time of day, and we averaged the histograms over monthly and seasonal time periods. The results are interpreted within the framework of a random model for cloud base height that we will describe.

Methodology

To generate the cloud base height frequency-of-occurrence histograms, we first processed the micro pulse lidar data with a cloud detection algorithm that is similar to the one described by Clothiaux et al. (1997) to produce estimates of the cloud base heights. For cloud base heights below 3 km, we used the Belfort ceilometer data because of its higher spatial resolution. To allow a significant number of observations to be contained in a time-height bin, we used 2-hr bin widths across a day and height bins centered at 0.5, 2.0, 4.0, 6.5 and 10 km with widths of 1, 2, 2, 3 and 4 km, respectively. The final cloud base height frequency-of- occurrence histograms were normalized by the total number of observations, both clear and cloudy, over the relevant interval of a month or a season to produce probability distributions of cloud base height occurrence as a function of time of day.

As an aid to the interpretation of the cloud base height frequency-of-occurrence histograms, consider the results of a simple stochastic model for the vertical distribution of cloud base heights. For each model realization of a vertical distribution of cloud, we assume that anywhere from one to four distinct layers can occur with equal probability. The cloud base heights of each layer are chosen at random

between 0 and 12 km. The lowest cloud base height of each realization is placed in the appropriate bin using the layers defined above, and we generate independent realizations (approximately 100 total) until the probability distributions of cloud base height as a function of time converge. The resulting distributions of cloud base height decrease exponentially and have an e-folding scale of approximately 2.25 km (Figure 1). This scale height of 2.25 km is sensitive to the maximum number of cloud layers that are possible in a given realization, as well as to their probability of occurrence; however, the exponential shape of the distribution is a robust feature of the model. Even though this simple model has no physical basis, it does provide a reasonable benchmark against which we can compare the observations.

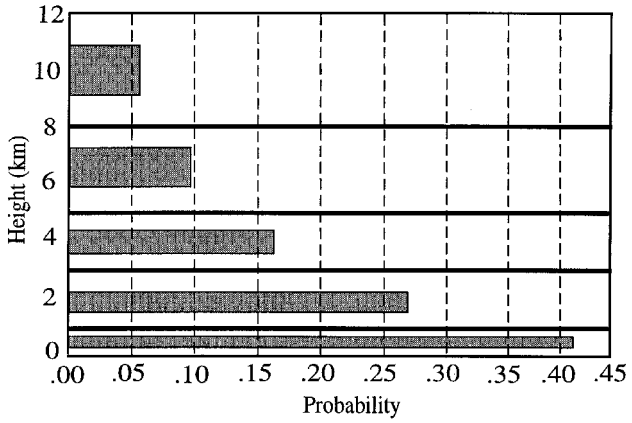

Figure 1. The vertical distribution of cloud base height predicted by the random model for cloud base height. The distribution is dominated by cloud base heights in the lowest km; the probability of cloud occurrence decreases exponentially with height and has a vertical scale height of 2.25 km. The heavy solid lines denote the boundaries of the height bins used to generate the histograms.

Results

The period of micro pulse lidar data from April 1994 to Spring 1995 contains over half a million observations, with approximately 43,200 observations per month. The simplest statistic that can be derived from the probability distributions of cloud base height as a function of the time of day is the fraction of observations that are cloudy (Figure 2).

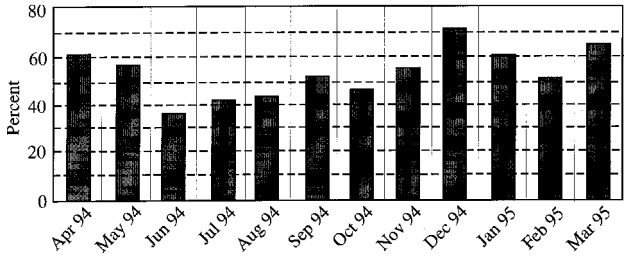

Figure 2. The percentage of the total observations for each month that indicated the presence of clouds at some height in the atmosphere.

Because the lidar probes only a narrow vertical column within the atmosphere, the statistic depicted in Figure 2 does not necessarily represent the spatial cloud fractional coverage. However, given the continuous nature of the observations and the relatively flat terrain around the site, it is likely that there is a high degree of correlation between the number of lidar cloudy observations and the actual spatial cloud fractional coverage. An annual cycle in the frequency of occurrence of cloudy lidar observations is clearly evident in Figure 2. The frequency decreases from just over 60% of all observations during April 1994 to an annual minimum of 35% during June 1994. The cloud fraction increases gradually during the next six months, reaching a maximum of just over 70% during December 1994. The frequency decreases during January and February 1995 and finally increases to 65% of all observations during March 1995.

In addition to the changes in the monthly frequency of occurrence of cloudy observations, there are also changes in the vertical distribution of cloud base heights from one season to the next (Figure 3). The vertical distribution of cloud base heights derived from the random model (Figure 1) is also illustrated in Figure 3; it is adjusted for the seasonal frequency of occurrence of cloudy observations. With the exception of summer 1994, the vertical distribution of cloud base heights does tend to decrease exponentially with height, up through the middle tropospheric bin centered at 4 km. The scale height of this exponential decrease, however, is greater than the scale height derived from the random model. Above the 4-km bin, the observed distribution of cloud base heights no longer decreases and may actually increase. Upper tropospheric clouds demonstrate little change in frequency of occurrence during the course of this particular annual cycle.

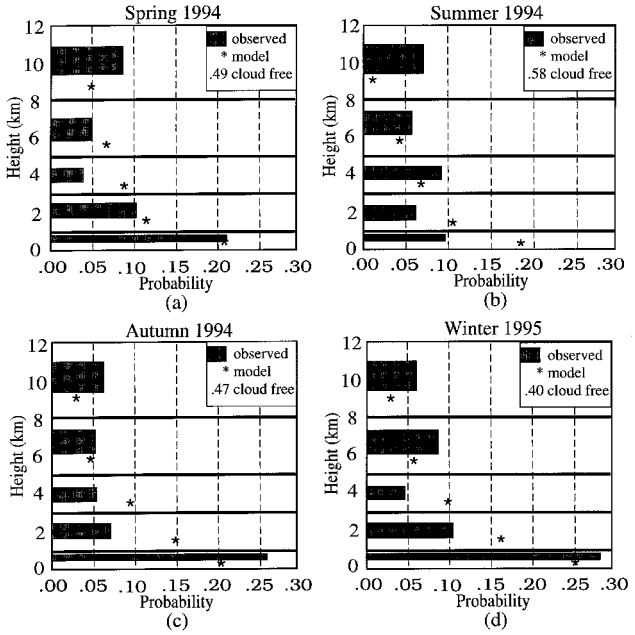

Figure 3. The vertical distribution of cloud base height observed by the micro pulse lidar and Belfort ceilometer for the four seasons. The dark shaded bars represent the data and the asterisks represent the random model prediction adjusted by the fraction of cloudy observations.

We have demonstrated to this point that 1) cloud base height frequency of occurrence, as observed from the surface, tends to be dominated by clouds in the lowest few km; 2) the vertical distribution of cloud base height decreases rapidly with height, much like the results produced by the random model for the distribution of cloud base heights; and 3) clouds in the upper troposphere are a major component of the cloud record over this site during this annual cycle. The seasonally averaged diurnal cycle of the probability of a cloudy observation is illustrated in Figure 4. Both spring and summer 1994 reveal a semidiurnal oscillation with peak probabilities of cloud occurrence around local noon; smaller local maxima in the probabilities occur near midnight during the spring and 0400 LST during the summer. The diurnal cycle for each height bin (not shown in the figure) reveals that the noon maximum is due to peaks in the 0.5 and 2 km height bins. During spring, the secondary maximum near midnight is caused by cirrus clouds above 8 km, while the summer peak near 0400 LST is due to an increase in cloudiness in the 3- to 5- km layer. Even though the fall and winter exhibit no strong overall diurnal cycle in total cloudiness (Figure 4), the cloud base height frequency of occurrences below 1 km tend to

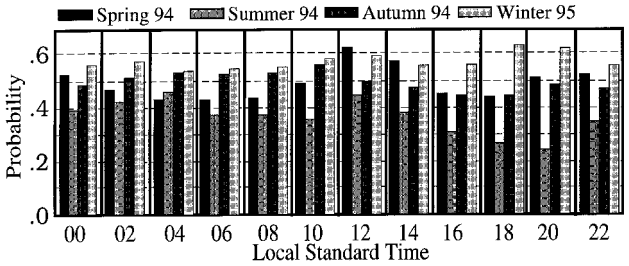

Figure 4. The diurnal cycle of cloud frequency of occurrence for each of the four seasons. The temporal bins are 2 hours wide and are centered on the odd hours.

peak broadly between 0600 LST and noon, and then decrease gradually during the afternoon and night. As the cloud base height frequency of occurrence in the lowest few kilometers decreases, the frequencies of occurrence in all higher bins increase.

Discussion and Conclusions

These preliminary results represent the initial compilation of a long-term cloud climatology derived from surface-based active remote sensors at the DOE ARM SGP central facility. As instruments of this type become more common and datasets from them become more extensive, accurate monitoring of the vertical distribution of cloudiness will become a reality, enhancing our ability to detect interannual variability and long-term trends in cloudiness. While we chose to examine the combined micro pulse lidar and Belfort laser ceilometer data in isolation from other cloud observations, the value of these datasets is enhanced by merging them with observations from satellite and ground-based cloud radar. A long-term satellite-lidar-radar cloud climatology will be extremely useful for validation of the parameterizations of clouds in large-scale atmospheric models. Even without the addition of satellite or cloud radar observations, the statistical distributions described above can be generated easily within a general circulation model and the modeled statistics compared directly to the observed statistics. This type of comparison is a necessary step in improving the characterization of cloudiness in climate models.

References

Clothiaux, E. E., G. G. Mace, T. P. Ackerman, T. J. Kane, J. D. Spinhirne, and V. S. Scott, 1997: An automated algorithm for detection of hydrometeor returns in micro pulse lidar data. *J. Atmos. Oceanic Technol*., submitted.

Clothiaux, E. E., M. A. Miller, B. A. Albrecht, T. P. Ackerman, J. Verlinde, D. M. Babb, R. M. Peters, and W. J. Syrett, 1995: An evaluation of a 94-GHz radar for remote sensing of cloud properties. *J. Atmos. Oceanic Technol*., **12**, 201-229.

Kropfli, R. A., S. Y. Matrosov, T. Uttal, B. W. Orr, A. S. Frisch, K. A. Clark, B. W. Bartram, R. F. Reinking, J. B. Snider, and B. E. Martner, 1995: Cloud physics studies with 8mm wavelength radar. *Atm. Research*, **35**, 299-313.

Reagan, J. A., M. P. McCormick, and J. D. Spinhirne, 1989: Lidar sensing of aerosols and clouds in the troposphere and stratosphere. *Proc. IEEE*, **77**, 433-448.

Uttal T., E. E. Clothiaux, T. P. Ackerman, J. M. Intrieri, and W. L. Eberhard, 1995: Cloud boundary statistics during FIRE II. *J. Atmos. Sci*., **52**, 4276-4284.

Winker, D. M., and M. A. Vaughn, 1994: Vertical distribution of clouds over Hampton, Virginia, observed by lidar under the ECLIPS and FIRE ETO Programs. *Atm. Research*, **34**, 117-133.